

1 **Title:** A novel method to selectively elicit cold sensations without touch

2

3 **Article type:** short communication

4

5 **Author names and affiliations:**

6 Ivan Ezquerra-Romano<sup>1</sup>

7 Maansib Chowdhury<sup>1</sup>

8 Caterina Maria Leone<sup>2</sup>

9 Gian Domenico Iannetti<sup>3, 4</sup>

10 Patrick Haggard<sup>1</sup>

11

12 1 Institute of Cognitive Neuroscience, University College London, London,

13 United Kingdom

14 2 Department of Human Neuroscience, Sapienza University, Rome, Italy

15 3 Division of Biosciences, University College London, London, UK

16 4 Neuroscience and Behaviour Laboratory, Italian Institute of Technology,

17 Rome, Italy

18

19 **Corresponding author:**

20 - p.haggard@ucl.ac.uk

21

22 **Highlights (4 points)**

23 Most studies on cold sensation fail to control for concomitant tactile input.

24 A method to deliver non-tactile cooling stimuli was developed.

25 The method combines dry ice, a thermal camera, and motorised stages.

26 The method delivers rapid ramps and feedback-controlled pulses.

27 Thresholds for contactless cold perception were estimated in humans.

28

29 **Abstract (250 words)**

30

31 *Background:* Thermal and tactile stimuli are transduced by different receptor classes.  
32 However, mechano- and thermo-sensitive afferents interact at spinal and supraspinal  
33 levels. Yet, most studies on responses to cooling stimuli are confounded by  
34 mechanical contact, making these interactions difficult to isolate. Methods for precise  
35 control of non-mechanical thermal stimulations remain challenging, particularly in the  
36 cold range.

37

38 *New Method:* We developed a non-tactile, focal, temperature-controlled, multi-  
39 purpose cooling stimulator. This method controls the exposure of a target skin region  
40 to a dry-ice source. Using a thermal camera to monitor skin temperature, and  
41 adjusting the source-skin distance accordingly, we could deliver non-tactile cooling  
42 stimuli with customisable profiles, for studying different aspects of cold sensation.

43

44 *Results:* To validate our method, we measured absolute and relative thresholds for  
45 cold sensation without mechanical contact in 13 human volunteer participants, using  
46 the method of limits. We found that the absolute cold detection threshold was  
47  $32.71^{\circ}\text{C} \pm 0.88^{\circ}\text{C}$ . This corresponded to a threshold relative to each participant's  
48 baseline skin temperature of  $-1.08^{\circ}\text{C} \pm 0.37^{\circ}\text{C}$ .

49

50 *Comparisons with Existing Method:* Our method allows cooling stimulation without  
51 the confound of mechanical contact, in a controllable and focal manner.

52

53 *Conclusions:* We report a non-contact cooling stimulator and accompanying control  
54 system. We used this to measure cold thresholds in the absence of confounding  
55 touch. Our method enables more targeted studies of both cold sensory pathways,  
56 and of cold-touch interactions.

57

58 **Keywords:**

59

60 Thermoception; Perception; Sensation; Temperature; Mechanosensation; Cold

61

## 62 **1 Introduction**

63

64 The first step of thermoception is the activation of free nerve endings in the  
65 epidermis. However, contact thermal stimuli unavoidably coactivate deeper, touch-  
66 related afferents. These tactile signals interfere with thermonociceptive input both at  
67 spinal and supraspinal levels (Cahusac & Noyce, 2007; Ho et al., 2011; Mancini et  
68 al., 2015). As a result, both physiological and psychophysical responses to  $\Delta$   
69 cooling-responsive units are confounded with tactile inputs, and quite possibly  
70 modulated by them. Therefore, cooling-mechanical co-stimulation precludes the  
71 study of non-tactile cooling responses. Yet, most research on cooling responses has  
72 used mechanical contact stimulators (e.g. Duclaux et al., 1974; Green, 2009). The  
73 logical way to study these interactions would involve comparing the effects of a  
74 cooling stimulus with the effects of a combined cooling and mechanical stimulus.

75

76 Therefore, studies of cold sensation would benefit from a cooling stimulation  
77 technique, which does not involve skin contact and mechanoreceptor activation such  
78 as laser stimulation in research on warm sensations (Iannetti et al., 2004). This  
79 technique would in turn allow interactions between cold and other sensations to be  
80 studied. Previous studies have attempted non-tactile cooling with stimulators that  
81 use ultrasound, chemicals, air flow or dry ice (CO<sub>2</sub> solid form). These approaches  
82 have some advantages, but importantly have limitations for studying interactions  
83 between mechanical and cooling signals in the context of sensory binding and object  
84 perception.

85

86 A recent study presented a new method to cool the skin with a non-contact tactile  
87 display driven by ultrasound waves (Nakajima et al., 2021). While this method allows  
88 precise spatial and temporal control of the cooling stimulation, it does not selectively  
89 elicit cold sensations because ultrasounds generate vibrotactile sensations. In  
90 contrast, chemical approaches (e.g. menthol) specifically elicit cold sensations  
91 without mechanical pressure, but controlling the duration and intensity of chemically-  
92 induced sensations is limited (Typolt & Filingeri, 2020). Non-contact methods based  
93 on blowing chilled air at tissues allow precise control of the duration, area and  
94 intensity of stimuli, but involve a certain level of air pressure that presumably  
95 stimulate mechano-sensitive afferents (Murphy et al., 2001; Bujas, 1937). Radiation  
96 or convection methods might achieve cooling without activation of tactile afferents.  
97 However, studies which have achieved temperature decrease of the skin using  
98 radiation and/or passive convection transfer between dry ice and the skin lacked

99 precise spatial and temporal control (Cataldo et al. 2016; Ferrè et al., 2018; Hardy &  
100 Oppel, 1938). Thus, they could not produce point-estimates of cold perceptual  
101 sensitivity of the kind used in psychophysical perceptual testing.

102

103 We have therefore developed a non-tactile, focal, temperature-controlled, multi-  
104 purpose cooling stimulator suitable for psychophysical testing on the perceptual  
105 aspect of cold sensation. Here, we describe three potential stimulation scenarios  
106 using this system. We validated our system in a study of human thresholds for cold  
107 perception in the absence of touch.

## 108 **2 Materials and methods**

109

110 To deliver non-tactile cooling stimulation, we used dry ice (CO<sub>2</sub>). The dry ice was  
111 held in a container, which varied in shape and dimension (10-2000 mL) according to  
112 the experimental application. The container was secured on a wooden support  
113 (30x2x2 cm), which could be moved in three axes using motorised linear stages (Fig.  
114 1A) (A-LSQ150B and X-LSQ150B series, Zaber Technologies Inc.). To control the  
115 time of exposure of the skin to the dry ice, we placed a polystyrene shutter below the  
116 syringe tip, and controlled the shutter with a servo motor (SG90 Micro Servo Motor  
117 KY66-5, Longruner), driven by an Arduino Mega 2560. The shutter was closed  
118 between trials. To measure the temperature of the skin immediately below the  
119 syringe tip, we used a thermal camera (module temporal resolution: 8.7 Hz, Field of  
120 View: 57° & camera resolution: 60 x 120) (Lepton 3.5, Teledyne FLIR), interfaced  
121 with a computer through a I/O module (PureThermal 2 - FLIR Lepton I/O Smart  
122 module, Teledyn FLIR).

123

124 To stimulate different skin regions during the same experiment, we had to control the  
125 position of the thermal camera. We used a second set of 3 motorised linear systems  
126 (2 stepper motor controllers LSM100B-T4 and 1 stepper motor controller LSM200B-  
127 T4, Zaber Technologies Inc.), which interfaced with the computer through controllers  
128 (2 stepper motor controllers X-MCB2 and 1 stepper motor controller X-MCB1, Zaber  
129 Technologies Inc.). These moved the thermal camera under computer control.

130

131 The motorised linear systems were positioned relative to the participant's left hand.  
132 Three red lasers (5V 650nm 5mW, HiLetgo®) fixed to the wall pointed at the hand  
133 dorsum. The participant's skin was marked with ink at the beam locations, so the  
134 experimenter could visually monitor the position of the participant's hand throughout  
135 (Fig. 1A). To control the hardware, build the experiment and analyse the data, we  
136 wrote custom Python and Arduino code (see software repository:  
137 <https://github.com/ieqrom/publication-cold-sensation-without-touch>).

138

139 Using these general principles, we realised three separate stimulation scenarios  
140 suitable for psychophysical and neurophysiological experiments. Here, we do not  
141 report combining these scenarios, but in principle they could be combined to realise  
142 other scenarios. Firstly, we developed a focal cooling stimulus to measure cold  
143 thresholds relative to baseline. Secondly, we developed a temperature feedback-  
144 controlled Proportional-Integral-Derivative (PID) solution for delivering prolonged  
145 customised cooling profiles. Thirdly, we produced a wide area rapid-cooling thermal  
146 pulse, designed to investigate cooling-evoked EEG potential. Finally, to validate our

147 method, we collected psychophysical data for scenario 1 and stimulation data from  
148 scenarios 2 and 3.

149

## 150 **2.1 Scenario 1: Focal cooling stimulation for cold threshold measurements**

151

152 In this scenario the dry ice was contained in a 10-ml syringe with a 4-cm blunt needle  
153 (BD Emerald Hypodermic Syringe - Luer Slip Concentric, BD). The syringe was  
154 wrapped in aluminium foil to reduce thermal loss. To obtain a constant pressure on  
155 the dry ice powder throughout, a weight of 1600 g was placed on the syringe plunger  
156 and a continuous rotation servo (FS5106R, Feetech) pressed on the plunger and the  
157 weight via a 3D printed linear system (Fig. 1A).

158

159 Thermal image recording started 2 s before the shutter opened. After shutter  
160 opening, the skin immediately below the syringe tip was exposed to convection of  
161 cooled air cooled by the dry ice (Appendix B). Further, the skin lost heat to the  
162 cooled syringe by radiation. As a result, the skin temperature gradually decreased,  
163 as recorded by the thermal camera. A region of interest (ROI, Fig. 1A & E) under the  
164 syringe tip was selected for online image analysis. Because the thermal camera was  
165 located slightly to the side of the syringe, and therefore had an oblique view, the  
166 circular ROI in the image had an elliptical projection (3.4x3.3 mm) on the skin. The  
167 pixel values in degrees Kelvin (K) were transformed into degrees Celsius ( $^{\circ}\text{C}$ ) and  
168 the temperature of the ROI was obtained by performing the mean across all the  
169 pixels within the ROI.

170

171 The capacity of the device to cool the skin decreases as the distance from the tip of  
172 the needle to the skin increases. We constructed a linear regression model  
173 (Appendix A) for selecting an appropriate distance to achieve the desired  
174 temperature range. For this scenario, we used a 5-cm distance.

175

176 To measure cold thresholds, we used the method of limits. At the start of each trial, a  
177 tone alerted the participant, and the shutter opened at the same time, exposing the  
178 participant's skin to the dry ice, and leading to a progressive decrease of the  
179 measured temperature in the ROI. The participant was instructed to press a foot  
180 pedal when they first felt a cold sensation on the stimulated skin region. When the  
181 pedal was pressed, the stimulator shutter closed, the tone terminated, and the final  
182 skin temperature was stored (Fig. 1E). To allow skin temperature to return to  
183 baseline, 4 locations were randomly stimulated. The locations were arranged in a  
184 square grid with a spacing of 2 cm. The same location was restimulated only after 2  
185 other locations had been visited, ensuring a minimum of 30 s for thermal recovery  
186 between stimulations at each site.

187

188 As well as measuring the absolute threshold, we used the data from each trial to  
189 calculate the relative threshold, i.e., the smallest drop in temperature from baseline  
190 that the participant could detect ( $\Delta T$ ) (Hafner et al., 2015). Unlike contact thermal  
191 stimulators, our stimulator does not set the initial temperature of the skin before each  
192 stimulation like the lasers used in the study of heat sensation (Iannetti et al., 2004).  
193 We observed variability (mean:  $33.8 \pm 0.9$   $^{\circ}\text{C}$  SD) in the baseline skin temperature  
194 across participants and grid locations. Because we only restimulated one location  
195 after at least 30 s, this variability is probably unrelated to the experimental  
196 procedure. Thus,  $\Delta T$  is arguably a more ecologically valid threshold measurement of

197 cold sensitivity than an absolute measurement. Our method and procedure are  
198 suited to account for this variability.

199

200 To measure  $\Delta T$ , an average of the baseline skin temperature within the ROI was  
201 taken across 26 frames in the 300 ms before shutter opening. Then, the temperature  
202 of the ROI upon pedal press was subtracted from the previous averaged baseline  
203 value to obtain  $\Delta T$  (Fig. 1B).

204

## 205 **Participants and ethics**

206

207 We measured cold thresholds on the hand dorsum of 13 participants (mean age:  
208  $24.1 \pm 3.5$  SD), obtaining 40 estimates per participant. Appropriate risk management  
209 procedures, notably around handling dry ice, were implemented. The research  
210 protocol was approved by the UCL Research Ethics Committee (ID number: ICN-  
211 PH-PWB-0847/010). Room temperature fluctuations and air currents were minimised  
212 by closing windows and doors.

213

214

## 215 **2.2 Scenario 2: Feedback temperature-controlled custom cooling stimulation**

216

217 This scenario allowed delivery of temperature-controlled non-tactile cooling  
218 stimulation for psychophysical paradigms which require long periods of constant low  
219 temperature. Raising the cooling source resulted in less cooling, while lowering it  
220 towards the skin produced more cooling. Therefore, to achieve the desired constant  
221 temperature reading from the thermal camera, we continuously adjusted the distance  
222 between dry ice and skin (Fig. 1C).

223

224 A PID algorithm closed the feedback loop between thermal image and the cooling  
225 source height above the skin. First, a desired temperature is set. Then, the thermal  
226 camera detects the temperature of a skin ROI, and a simple PID feedback controller  
227 sends position commands to the motorised linear system, adjusting the height of the  
228 container until the desired temperature is reached. This allows precise temporal and  
229 spatial control of skin temperature for psychophysical experiments. For instance, in  
230 combination with a non-tactile warm stimulator, a temperature-controlled radiant  
231 Thermal Grill Illusion (TGI) could be elicited for the first time.

232

233 In this set-up, the dry ice was held in a cardboard container. The cardboard container  
234 had dimensions 10.2x10.2x21.8 cm with a total volume of 1600 ml. It was filled with  
235 300 g of dry ice. The base was perforated with a 6-mm diameter copper tube. For  
236 these studies, the ROI had a projected elliptical shape on the skin of 5x4 mm. The  
237 interior of the container was covered with foil and its exterior with polystyrene foam in  
238 order to limit thermal loss and convection to the copper tube.

239

## 240 **2.3 Scenario 3: Rapid, wide-area, high-intensity cooling stimulation**

241

242 This scenario allowed delivery of fast non-tactile cooling stimulation of a large skin  
243 area, designed to produce a strong afferent volley and an evoked brain response.  
244 Event-related EEG potentials require such strong stimuli with rapid onsets. Steep  
245 cooling ramps cause synchronous activation of many cold afferents, and therefore

246 improve the signal-to-noise ratio of event-related EEG potentials, thus paralleling  
247 what has been demonstrated for steep radiant heating ramps (Iannetti et al., 2004).

248

249 In this set-up, the dry ice container for scenario 2 was used, but the base was  
250 perforated with three outlet tubes to increase the stimulation area. Therefore, the  
251 exposed skin area was larger, and the skin ROI was a 10x8 mm ellipse. Stimulation  
252 led to a rapid temperature decrease at  $13 \pm 3$  °C/s SD (Fig. 1D). Previous studies  
253 have shown that a cooling ramp of 10-17°C/s delivered to an 1444 mm<sup>2</sup> skin area is  
254 sufficient to detect a reproducible evoked potential (Duclaux et al., 1974). Thus, our  
255 stimulation method permits rapidly cooling a large patch of skin without touch, and  
256 potentially measuring the EEG responses elicited by cooling stimuli without  
257 mechanical input.

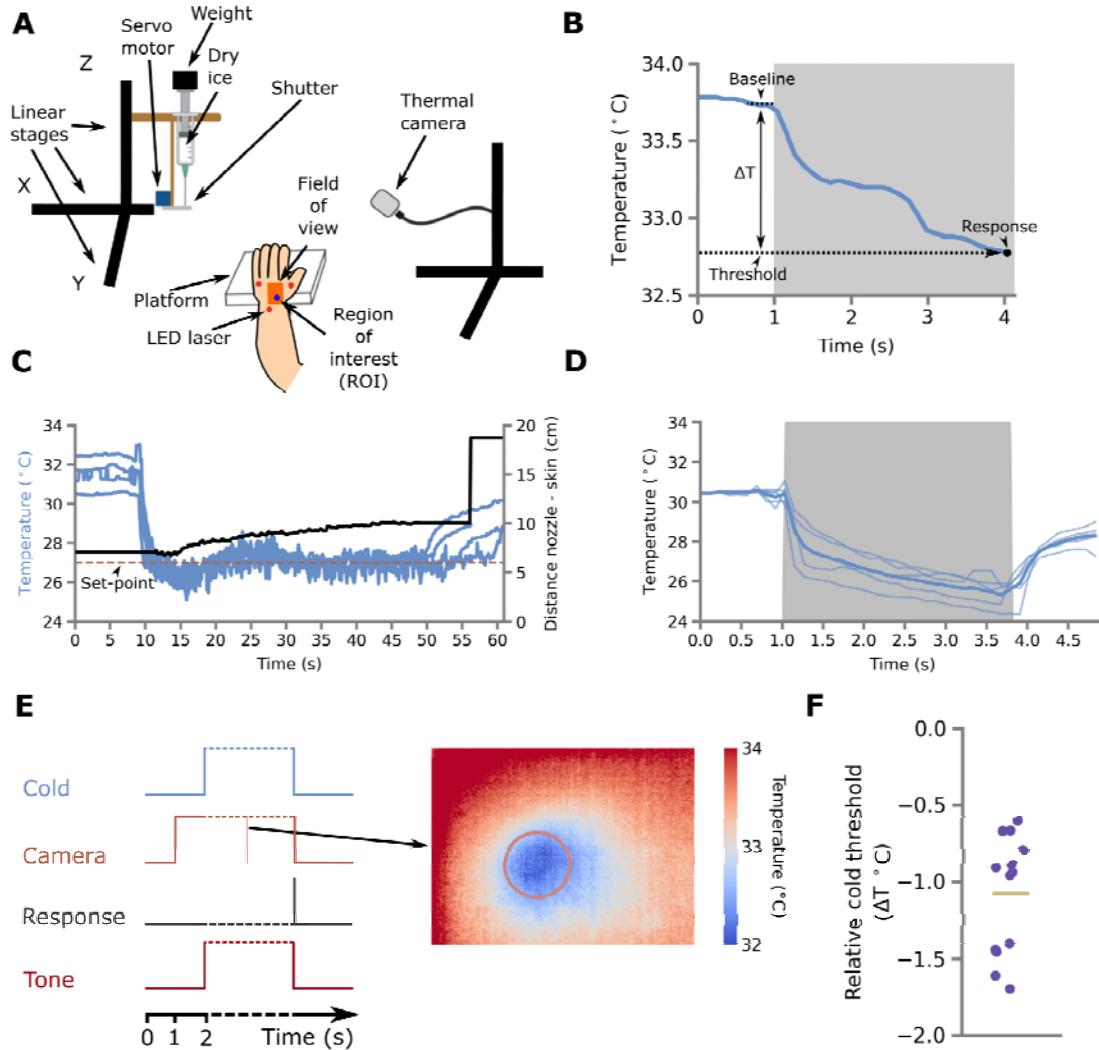
258

### 259 **3 Results**

260

261 Our stimulator successfully delivered cooling stimulation without touch. We  
262 determined absolute and relative temperature threshold of cold detection (Fig. 1B &  
263 F). We also achieved repeatable, sustained, temperature-controlled cooling  
264 stimulation suitable for psychophysical studies of cold perception with stimuli varying  
265 in intensity, location, and duration (Fig. 1C). Finally, we demonstrated a rapid  
266 decrease in skin temperature without touch, which is suitable for electrophysiological  
267 recordings (Fig. 1D).

268



269  
270  
271  
272  
273  
274  
275  
276  
277  
278  
279  
280  
281  
282  
283  
284  
285

**Fig. 1. A)** An illustration of the set-up with the main components. **B)** Example of focal cooling stimulation for determining cold thresholds by method of limits (scenario 1). The trace shows mean skin temperature in the skin ROI. The threshold level at which the participant first reported detecting cold is expressed relative to baseline ( $\Delta T$ ). The grey zone indicates the duration of cold stimulation (shutter is open). **C)** Example traces (blue lines,  $n=4$  repetitions) of feedback-controlled stimulation (scenario 2). The horizontal, dashed red line indicates the set-point for the PID controller. The height of the stimulator above the skin is adjusted by PID control to achieve the desired temperature (one illustrative trace is shown by the black line, referring to right-hand ordinate scale). **D)** Examples of rapid, large-area cooling ramps (thin blue lines,  $n=5$  normalised repetitions; scenario 3). The thick blue line shows the mean. **E)** The panel to the left is a schematic displaying the temporal sequence of events in an MoL trial. The panel to the right shows a thermal image during dry ice stimulation. The orange circle represents the ROI. **F)** Cold detection thresholds relative to baseline skin temperature ( $\Delta T$ ) of 13 participants. Each datapoint represents the mean of 40 threshold estimates based on the method of Fig. 1B. The horizontal yellow line represents the mean.

286 Baseline temperature before cooling stimulation was  $33.8 \pm 0.9$  °C SD across 13  
287 participants. The absolute threshold for reporting cooling stimulation was  $32.7 \pm 0.9$   
288 °C SD across participants. Thus, the relative threshold for cold detection ( $\Delta T$ ) was -  
289  $1.1 \pm 0.4$  °C across participants (Fig. 1F).

## 290 **4 Discussion**

291

292 We report a novel method to generate controlled and focal cooling stimulations  
293 without the confounds of mechanical input. We show how the system can be used to  
294 perform psychophysical experiments on the perceptual aspect of cold sensation. We  
295 have focussed on the methodological issues around non-contact cooling stimulation.  
296 Importantly, our approach overcomes some of the limitations of previous non-contact  
297 cooling approaches. Firstly, non-contact methods using ultrasound and air blow do  
298 involve mechanical stimulation (Bujas, 1937; Nakajima et al., 2021; Murphy et al.,  
299 2001). Secondly, previous studies using chemical and dry ice approaches to  
300 selectively elicit cold sensations had poor spatio-temporal controllability (Cataldo et  
301 al. 2016; Ferrè et al., 2018; Hardy & Oppel, 1938; Typolt & Filingeri, 2020).

302

303 Furthermore, we show that our method can be used for perceptual psychophysics.  
304 The most widespread cold perception test is the calculation of a cooling detection  
305 threshold using a method of limits. This is the basis of the cold threshold test  
306 performed in Quantitative Sensory Testing (QST) studies that are frequently used in  
307 clinical studies. The data from our device (Fig. 1F) showed cold thresholds close to  
308 the published normative values for QST using methods of limits (Rolke et al., 2006:  
309 30.9°C from 32°C baseline; Hafner et al., 2015: -1.0°C degrees). All these studies,  
310 however, used contact thermodes, thus introducing a tactile element. Here, we have  
311 shown that our method could reliably estimate focal cold detection thresholds without  
312 mechanical stimulation, which are comparable to existing normative values. This  
313 validates the use of our method for perceptual psychophysical experiments.  
314 Crucially, the duration and size of our cooling stimuli is unlikely to trigger homeostatic  
315 responses. Thus, our method is suitable for studying the perceptual aspect of cold  
316 sensation, but not its regulatory aspect.

317

318 Therefore, our non-tactile thermal cooling stimulator opens the possibility of  
319 investigating cold-touch interactions. The classic method to study such interactions  
320 would involve comparing the responses to thermal stimuli both with and without  
321 concomitant mechanoreceptor stimulation. However, the mechanisms of thermo-  
322 tactile interactions are poorly understood because most methods for delivering  
323 cooling stimulation involve mechanical stimulation. In future studies, our stimulator  
324 will be used to address the scientific question of how mechanical stimulation  
325 interacts with cooling stimulation. For example, cold thresholds could be measured in  
326 the presence or absence of concomitant touch. If an interaction between touch and  
327 thermal sensitivity is established, EEG studies could investigate the  
328 neurophysiological mechanisms underlying this interaction. Our rapid, large-scale  
329 cold stimulator could potentially allow future electrophysiological recordings of cold-  
330 evoked potentials, and of how they might be modulated by tactile input. Furthermore,  
331 future studies could combine scenarios to deliver more sophisticated thermal profiles  
332 such as PID-controlled ramps (scenarios 2 & 3). This combined scenario could be  
333 used to study cold perception for different temperature gradients without tactile input.

334

335

336 Our results of the cooling detection thresholds have some limitations. First, the  
337 method of limits does not distinguish between two key components of sensory  
338 detection: sensitivity and bias. Further, we did not include 'catch' trials, in which the  
339 auditory tone would occur without any cold stimulation. The absence of catch trials



340 could potentially induce a response bias, with participants responding based on the  
341 expectation that a cold sensation would occur. Thus, our measures of cold  
342 thresholds should not be taken as perfect estimates of sensitivity. However, this  
343 does not detract from the scientific value of the stimulator apparatus. Future studies  
344 could use psychophysical methods such as signal detection to estimate thermal  
345 sensitivity independent of bias.

346

347 In our method, two modes of heat transfer contribute to skin cooling: convection and  
348 radiation. Convection cooling takes place as sublimated CO<sub>2</sub> and cooled air flow  
349 down from the container to the skin because they are more dense than ambient air.  
350 Radiative cooling also transfers thermal energy from warmer objects (the skin) to  
351 cooler ones (the stimulator). Our design cannot distinguish the respective  
352 contributions of convection and radiation to skin cooling. The very focal cooling  
353 achieved in scenario 1 suggests that convection dominates. One might object that  
354 cold air currents flowing downwards to the skin constitute a mechanical stimulus, and  
355 that our method is not therefore completely non-tactile. We addressed this limitation  
356 by measuring the convection airflow in our exposure Scenario 1 with a Pitot tube,  
357 and calculating the resulting mechanical forces at the skin. The velocity of the airflow  
358 immediately below the syringe tip was measured as 4.0 m/s ± 0.30 SD (density of  
359 sublimated CO<sub>2</sub>: 1.836 kg/m<sup>3</sup>; MPXV7002DP pressure sensor, NXP). Calculations  
360 confirmed that the resulting forces on the skin were below published  
361 mechanoreceptor threshold values. Finally, in informal pilot testing, we gently blew  
362 air through the syringe at this velocity, and found that this level of airflow was not  
363 perceptually detectable (Appendix B). Therefore, our cooling stimulator could be  
364 considered having both high sensitivity (effectively stimulating cold afferents) and  
365 high specificity (not stimulating non-thermal afferents, notably mechanoreceptor  
366 afferents). However, further psychophysical and electrophysiological studies should  
367 investigate the sensitivity and specificity of our method.

## 368 **5 Conclusions**

369

370 We describe a novel non-tactile, focal, temperature-controlled, multi-purpose  
371 stimulator. We show how this device can be used for non-tactile thermal stimulation  
372 in humans. Future studies can use our stimulation method in different  
373 psychophysical and neurophysiological experiments to establish a thermo-tactile  
374 interaction. Understanding the mechanisms of thermo-tactile and thermo-thermal  
375 interactions would help improving clinical treatments, thermal displays and other  
376 haptic devices.

377

### 378 **Authors' contributions**

379

380 Ivan Ezquerra-Romano: Conceptualization, Methodology, Software, Data collection,  
381 Data curation, Visualization, Investigation, Writing - Original, Validation, Formal  
382 analysis, Investigation. Maansib Chowdhury: Data collection, Validation. Caterina  
383 Maria Leone: Conceptualization, Methodology, Draft, Writing – Review & Editing.  
384 Gian Domenico Iannetti: Conceptualization, Methodology, Funding, Supervision,  
385 Resources, Draft, Writing – Review & Editing. Patrick Haggard: Conceptualization,  
386 Methodology, Funding, Supervision, Writing – Review & Editing, Resources,  
387 investigation.

388 **Acknowledgements**

389 I.E.R. was supported by the Biotechnology and Biological Sciences Research  
390 Council (UK) [grant number BB/M009513/1]. M.C. was supported by a European  
391 Union Horizon 2020 Research and Innovation 385 Programme (TOUCHLESS,  
392 project No. 101017746). Additional funding was provided by a UCL ‘Cities  
393 Partnership Project’ grant, which supported C.M.L. and G.D.I. G.D.I. was supported  
394 by the ERC (PAINSTRAT grant). The authors would like to thank Martin Donovan for  
395 his technical support in the development of the methodology. Help from Dr. Shinya  
396 Takamuku was also greatly appreciated. Informal discussions with Angel Ezquerro  
397 and Guanhaven Romano-Mendoza were helpful in the inception and development of  
398 the methodology.

399

400 **Declaration of Competing Interests**

401

402 The authors declare no competing interests.

403 **References**

404

405 Bujas, Z. (1937). V. La sensibilité au froid en fonction du temps. *L'Année*  
406 *Psychologique*, 38(1), 140–147. <https://doi.org/10.3406/PSY.1937.5503>

407

408 Cahusac, P. M. B., & Noyce, R. (2007). A pharmacological study of slowly adapting  
409 mechanoreceptors responsive to cold thermal stimulation. *Neuroscience*, 148(2),  
410 489–500. <https://doi.org/10.1016/j.neuroscience.2007.06.018>

411

412 Cataldo, A., Ferrè, E. R., Di Pellegrino, G., & Haggard, P. (2016). Thermal referral:  
413 Evidence for a thermoceptive uniformity illusion without touch. *Scientific Reports*,  
414 6(September), 1–10. <https://doi.org/10.1038/srep35286>

415

416 Duclaux, R., Franzen, O., Chatt, A. B., Kenshalo, D. R., & Stowell, H. (1974).  
417 Responses recorded from human scalp evoked by cutaneous thermal stimulation.  
418 *Brain Research*, 78(2), 279–290. [https://doi.org/10.1016/0006-8993\(74\)90552-6](https://doi.org/10.1016/0006-8993(74)90552-6)

419

420 Ferrè, E. R., Iannetti, G. D., van Dijk, J. A., & Haggard, P. (2018). Ineffectiveness of  
421 tactile gating shows cortical basis of nociceptive signaling in the Thermal Grill  
422 Illusion. *Scientific Reports*, 8(1), 6584. <https://doi.org/10.1038/s41598-018-24635-1>

423

424 Green, B. G. (2009). Temperature perception on the hand during static versus  
425 dynamic contact with a surface. *Attention, Perception, and Psychophysics*, 71(5),  
426 1185–1196. <https://doi.org/10.3758/APP.71.5.1185>

427

428 Hafner, J., Lee, G., Joester, J., Lynch, M., Barnes, E. H., Wrigley, P. J., & Ng, K.  
429 (2015). Thermal quantitative sensory testing: A study of 101 control subjects. *Journal*  
430 *of Clinical Neuroscience*, 22(3), 588–591. <https://doi.org/10.1016/j.jocn.2014.09.017>

431

432 Hardy, J. D., & Opiel, T. W. (1938). Studies in temperature sensation. IV. The  
433 stimulation of cold sensation by radiation. *The Journal of Clinical Investigation*, 17(6),  
434 771–778. <https://doi.org/10.1172/JCI101007>

435

436 Ho, H.-H., Watanabe, J., Ando, H., & Kashino, M. (2011). Mechanisms Underlying  
437 Referral of Thermal Sensations to Sites of Tactile Stimulation. *Journal of*  
438 *Neuroscience*, 31(1), 208–213. <https://doi.org/10.1523/JNEUROSCI.2640-10.2011>

439

440 Iannetti, G. D., Leandri, M., Truini, A., Zambreanu, L., Cruccu, G., & Tracey, I.  
441 (2004). Aδ nociceptor response to laser stimuli: selective effect of stimulus duration  
442 on skin temperature, brain potentials and pain perception. *Clinical Neurophysiology*,  
443 115(11), 2629–2637.

444

445 Mancini, F., Beaumont, A. L., Hu, L., Haggard, P., Iannetti, G. D. (2015). Touch  
446 inhibits subcortical and cortical nociceptive responses, *PAIN*, 156(10), 1936–1944.  
447 <https://doi.org/10.1097/j.pain.0000000000000253>

448

449 Rolke, R., Baron, R., Maier, C. A., Tölle, T. R., Treede, R. D., Beyer, A., ... &  
450 Wasserka, B. (2006). Quantitative sensory testing in the German Research Network  
451 on Neuropathic Pain (DFNS): standardized protocol and reference values. *Pain*,  
452 123(3), 231–243. <https://doi:10.1016/j.pain.2006.01.041>

453

454 Nakajima, M., Hasegawa, K., Makino, Y., & Shinoda, H. (2021). Spatiotemporal  
455 Pinpoint Cooling Sensation Produced by Ultrasound-Driven Mist Vaporization on  
456 Skin. *IEEE Transactions on Haptics*, 14(4), 874-884.

457 <https://doi.org/10.1109/TOH.2021.3086516>

458

459 Typolt, O., & Filingeri, D. (2020). Evidence for the involvement of peripheral cold-  
460 sensitive TRPM8 channels in human cutaneous hygrosensation. *American Journal*  
461 *of Physiology-Regulatory, Integrative and Comparative Physiology*, 318(3), 579-589.

462 <https://doi.org/10.1152/ajpregu.00332.2019>

463

464 Murphy, P. J., Patel, S., Morgan, P. B., & Marshall, J. (2001). The minimum stimulus  
465 energy required to produce a cooling sensation in the human cornea. *Ophthalmic*  
466 *and Physiological Optics*, 21(5), 407-410. <https://doi.org/10.1016/S0275->

467 5408(01)00013-8

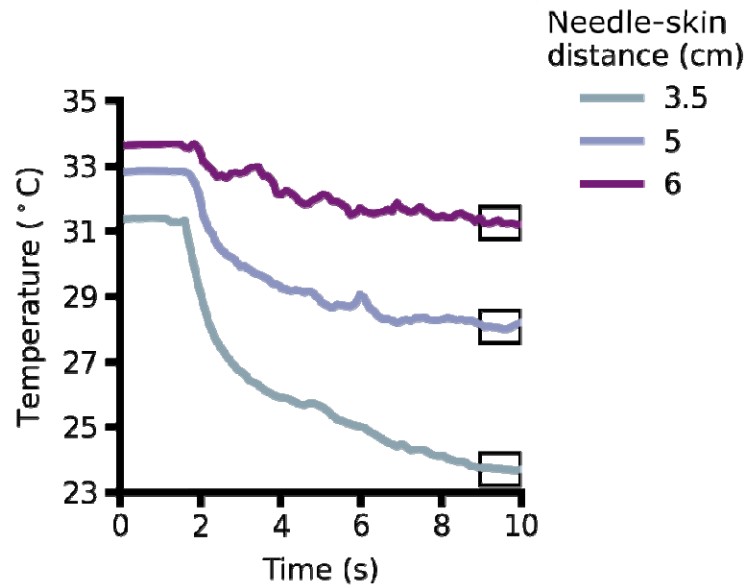
468

469

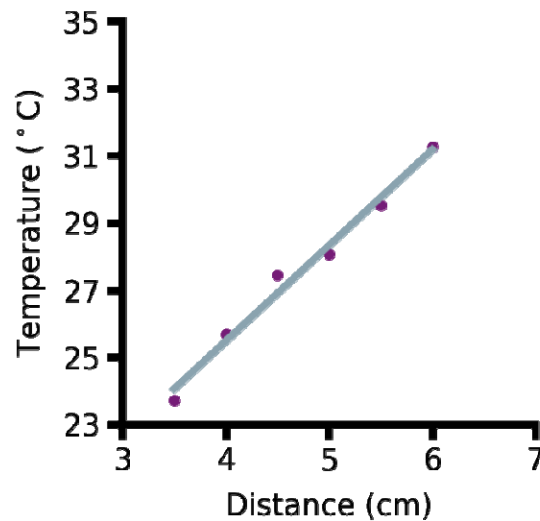
470 **Appendix A – Linear regression model**

471

**A**



**B**



472

473 **Linear regression model.** Thermal effects of distance between cold source and skin are  
474 used to create a linear regression model for obtaining feedforward stimulus parameters. A)  
475 Traces showing mean temperature of the skin ROI for 3 different distances between the  
476 needle's tip and the skin. Each trace is the mean of 5 recordings at the given distance. The  
477 grey zone indicates the duration of cold stimulation (shutter is open). The black open boxes  
478 over indicate the data used to calculate the model represented in Fig. B. B) Dots showing  
479 the final temperature at each distance and trace showing the linear fit. At 6 different  
480 distances, 5 recordings of the skin temperature during cold stimulation were made. After  
481 performing the mean of the traces at each distance, the mean temperature during the final  
482 1 s of stimulation was extracted (black box in Fig. A). A linear regression was used to model  
483 the relation between distance and temperature. The model could then be used to position  
484 the syringe either to allow a desired temperature to be reached, either using feedforward  
485 control, or as an initial estimate of distance for a feedback-controlled stimulation.

## 486 Appendix B. Airflow force and d' calculations.

487

### 488 Airflow force calculation

489

490 Dry ice is solidified CO<sub>2</sub>. It sublimates directly from its solid state below -80°C to a  
491 gaseous state at standard temperature and pressure. These characteristics make  
492 this material suitable for non-tactile cooling. The sublimation of dry ice produces  
493 airflow from the needle's tip of the syringe. To obtain the force that this airflow exerts  
494 on the skin, we use the following formula for fluid dynamics:

495

$$496 F = P * A \quad (\text{Formula 1}),$$

497

498 To calculate the force, we need to obtain the pressure (P) and the area (A) of the  
499 airflow when it collides with the skin.

500

501 In a fluid, the dynamic pressure is the kinetic energy per unit volume. To calculate  
502 the dynamic pressure, we can use the following formula:

503

$$504 p_D = \frac{1}{2} * \rho * v^2 \quad (\text{Formula 2}),$$

505

506 where  $\rho$  is the density of the fluid and  $v$  is the speed of the fluid. We used the density  
507 of CO<sub>2</sub> at standard room temperature (25 °C) and pressure (1 atm) -  $\rho = 1.84 \text{ kg/m}^3$ .  
508 The velocity of the jet of air was measured with a pitot tube. The pitot tube was  
509 placed at 5 cm below the tip of the needle, which is the distance at which the skin  
510 was during the experiment described in Fig. 1F. The mean velocity of the jet of air  
511 sampled at 10 Hz and averaged over a 4 s period was 4.06 m/s (SD 0.30 m/s).  
512 Therefore, following from Formula 1, the dynamic pressure that the jet of air exerts  
513 on the skin is:

514

$$515 p_D = \frac{1}{2} * 1.84 * 4.06^2 = 15.16 \frac{N}{m^2} .$$

516

517

518 To obtain the area of the airflow when it collides with the skin, we can use the ellipse  
519 drawn on the skin by the circular ROI taken from thermal camera measurements in  
520 scenario 1. The cooled area of the skin was measured as an ellipse with axis lengths  
521 3.37 mm and 3.32 mm. The area of an ellipse is:

522

$$523 A = \pi * a * b \quad (\text{Formula 3}).$$

524

525 Therefore, the area cooled in scenario 1 was,

526

$$527 A = \pi * 3.32 \text{ mm} * 3.37 \text{ mm} = 3.52 \times 10^{-5} \text{ m}^2 .$$

528

529 Following from Formula 1, the force that the jet of air exerts on the skin is:

530

$$531 F = P * A = 0.53 \text{ mN} ,$$

532

533 The estimated threshold for exciting a single mechanoreceptor afferent by punctate  
534 stimulation of glabrous skin was estimated using microneurography (Johansson et

535 al., 1980). They found that RA units had a median threshold of 0.58 mN. PC units  
536 had a median threshold of 0.54 mN. Slowly adapting SAI and SAI units had median  
537 values of 1.3 mN and 7.5 mN, respectively. In our setup, convection currents from  
538 the cold source may be assumed constant. Therefore, the mechanoreceptor  
539 afferents most likely to be stimulated are the SAI units. Therefore, the mechanical  
540 element of our cold stimulation is less than half the force level suggested to trigger a  
541 single mechanoreceptor afferent action potential. We therefore conclude that  
542 convection currents from our cold stimulator were unlikely to produce any effective  
543 mechanical stimulation.

544

## 545 **D' for the detection of airflow**

546

547 To further assess whether the mechanical stimulation generated by the minimal  
548 airflow during our main experiment was perceptually detectable, we performed a pilot  
549 Signal Detection Theory experiment.

550

551 The experimenter blew through the syringe on a participant's forearm. In 10 trials,  
552 the syringe was perpendicular to the skin and at distance of 5 cm (stimulus present).  
553 In another 10 trials, the syringe was moved away so that the participant's arm was  
554 not stimulated (stimulus absent). The participant was asked to detect the jet of air.  
555 For this experiment, 4 naïve, blindfolded participants were tested.

556

557 Before performing the experiment, the experimenter was trained to blow through the  
558 syringe to generate a jet of air with a velocity of 5.09 m/s as recorded by the Pitot  
559 tube. Therefore, the airflow of atmospheric air (density: 1.204 kg/m<sup>3</sup>) produced a  
560 force of 0.55 mN.

561

562 On average, the hit rate was 26% and the false alarm rate was 15%. Across 4  
563 participants, D' was 0.53 and the criterion response (c) was -0.94. This pilot  
564 psychophysical test suggests that the level of airflow (speed and area) generated by  
565 the syringe with dry ice was below perceptual detection threshold for  
566 mechanoreceptor sensations.

567

568

## 569 **References**

570

571 Johansson, R. S., Vallbo, Å. B., & Westling, G. (1980). Thresholds of  
572 mechanosensitive afferents in the human hand as measured with von Frey  
573 hairs. *Brain Research*, 184(2), 343–351. [https://doi.org/10.1016/0006-](https://doi.org/10.1016/0006-8993(80)90803-3)  
574 8993(80)90803-3

575

576

577